University of Massachusetts Amherst

From the SelectedWorks of Daiheng Ni

2012

Vehicle Longitudinal Control and Traffic Stream Modeling (Paper # 12-0156)

Daiheng Ni, *University of Massachusetts - Amherst*
John D. Leonard
Gabriel Leiner
Chaoqun Jia

Available at: https://works.bepress.com/daiheng_ni/8/

Vehicle Longitudinal Control and Traffic Stream Modeling

Daiheng Ni, Ph.D. (corresponding author)
Assistant Professor
Department of Civil and Environmental Engineering,
University of Massachusetts Amherst
130 Natural Resources Road
Amherst, MA 01003, USA
Phone: (413) 545-5408
Fax: (413) 545-9569
E-mail: ni@ecs.umass.edu

John D. Leonard, Ph.D.
Associate Dean and Associate Professor
College of Engineering
Georgia Institute of Technology
Atlanta, GA 30332
Phone: (404) 894-3482
Email: john.leonard@coe.gatech.edu

Gabriel Leiner
Graduate student
University of Massachusetts Amherst
130 Natural Resources Road
Amherst, MA 01003, USA
E-mail: gleiner@engin.umass.edu

Chaoqun (Enzo) Jia
Graduate student
University of Massachusetts Amherst
130 Natural Resources Road
Amherst, MA 01003, USA
E-mail: cjia@engin.umass.edu

6000 words + 11 figures + 2 tables

January 10, 2012

Abstract

A simple yet efficient traffic flow model, in particular one that describes vehicle longitudinal operational control and further characterizes traffic flow fundamental diagram, is always of great interest to many. Though many models have been proposed in the past, each with their own advantages, research in this area is far from conclusive. This paper contributes a new model, i.e., the longitudinal control model (LCM), to the arsenal with a unique set of properties. The model is suited for a variety of transportation applications, among which a concrete example is provided herein.

Keywords: Mathematical modeling, traffic flow theory, car following, fundamental diagram

1 Introduction

A simple yet efficient traffic flow model, in particular one that describes vehicle longitudinal operational control and further characterizes traffic flow fundamental diagram, is always of great interest to many. For example, researchers can use such a model to study traffic flow phenomena, system analysts need the model to predict system utilization and congestion, accident investigators find the model handy to reconstruct accidents, software developers may implement the model to enable computerized simulation, and practitioners can devise strategies to improve traffic flow using such a simulation package.

Past research has resulted in many traffic flow models including microscopic car-following models and macroscopic steady-state models, each of which has its own merits and is applicable in a certain context with varying constraints. A highlight of these historical efforts will be provided later in Section 6. Nevertheless, research on traffic flow modeling is far from conclusive, and a quest for better models is constantly occurring. Joining such a journey, this paper presents a new model, the longitudinal control model (LCM), as a result of modeling from a combined perspective of Physics and Human Factors (Section 2). The model seems to possess a unique set of properties:

- The model is *physically meaningful* because it captures the essentials of longitudinal vehicle control and motion on roadways with the presence of other vehicles (Subsection 2.1)
- The model is *simple* because it uses one equation to handle all driving situations in the longitudinal direction (Equation 2), and this microscopic equation aggregates to a steady-state macroscopic equation that characterizes traffic stream in the entire density range (Equation 5)
- The model is *flexible* because the microscopic equation provides the mechanism to admit different safety rules that govern vehicle driving (Subsection 2.1) and the macroscopic equation has the flexibility to fit empirical traffic flow data from a variety of sources (Subsection 3.2 and Figures 3 through 8)
- The model is *consistent* because the microscopic equation aggregates to the macroscopic equation so that the micro-macro coupling is well defined (Subsection 2.2). As a result, traffic flow modeling and simulation based on the microscopic model aggregates to predictable macroscopic behavior (Section 5, see how results of microscopic and macroscopic approaches match)
- The model is *valid* as verified using field observations from a variety of locations (Section 4), and the model is realistic as demonstrated in an example application (Section 5)

The unique set of properties possessed by the LCM lend itself to various transportation applications including those mentioned above. An example of such applications is elaborated in Section 5 where the LCM is applied to analyze traffic congestion macroscopically and microscopically. Research findings are summed up in Section 7.

2 The Longitudinal Control Model

Vehicle operational control in the longitudinal direction concerns a driver's response in terms of acceleration and deceleration on a highway without worrying about steering including lane changing. Rather than car-following as it is conventionally termed, vehicle longitudinal control involves more driving regimes than simply car-following (e.g. free flow, approaching, stopping, etc.). A field theory was previously proposed [1], [2], which represents the environment (e.g. the roadway and other vehicles) perceived by a driver with ID i as an overall field U_i. As such, the driver is subject to forces as a result of the field. These forces, which impinge upon the driver's mentality, are motivated as roadway gravity G_i, roadway resistance R_i, and vehicle interaction F_i^j with the leading vehicle j, see an illustration in Figure 1. Hence, the driver's response is the result of the net force $\sum F_i$ acting on the vehicle according to Newton's second law of motion:

$$\sum F_i = G_i - R_i - F_i^j \tag{1}$$

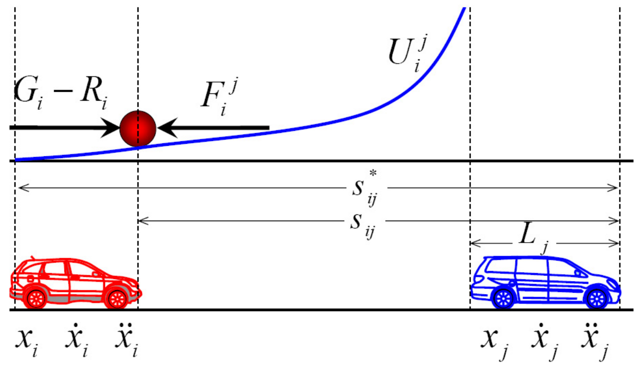

Figure 1: Forces acting on a vehicle

2.1 *Microscopic model*

If the functional forms of the terms in Equation 1 are carefully chosen (mainly by experimenting with empirical data), a special case called the Longitudinal Control Model (LCM) can be explicitly derived from Equation 1 as :

$$\ddot{x}_i(t+\tau_i) = A_i[1 - (\frac{\dot{x}_i(t)}{v_i}) - e^{1-\frac{s_{ij}(t)}{s_{ij}^*(t)}}] \tag{2}$$

where $\ddot{x}_i(t+\tau_i)$ is the operational control (acceleration or deceleration) of driver i executed after a perception-reaction time τ_i from the current moment t. A_i is the maximum acceleration desired by driver i when starting from standing still, $\dot{x}_i$ is vehicle i's speed, v_i driver i's desired speed, s_{ij} is the actual spacing between vehicle i and its leading vehicle j, and s_{ij}^* is the desired value of s_{ij}.

No further motivation for this special case is provided other than the following claims: (1) it takes a simple functional form that involves physically meaningful parameters but not arbitrary coefficients (see this and the next section), (2) it makes physical and empirical sense (see this and Section 4), (3) it provides a sound microscopic basis to aggregated behavior, i.e. traffic stream modeling (see the remainder of this section and Section 4), and (4) it is simple and easy to apply (see Section 5).

The determination of desired spacing $s_{ij}^*(t)$ admits safety rules. Basically, any safety rule that relates spacing to driver's speed choice can be inserted here. Of particular interest is an algorithm for desired spacing that allows vehicle i to stop behind its leading vehicle j after a perception-reaction time τ_i and a deceleration process (at rate $b_i > 0$) should the leading vehicle j applies an emergency brake (at rate $B_j > 0$). After some math, the desired spacing can be determined as:

$$s_{ij}^*(t) = \frac{\dot{x}_i^2(t)}{2b_i} - \frac{\dot{x}_j^2(t)}{2B_j} + \dot{x}_i\tau_i + l_j \tag{3}$$

where l_j is vehicle j's effective length (i.e., actual vehicle length plus some buffer spaces at both ends). Note that the term $\frac{\dot{x}_i^2(t)}{2b_i} - \frac{\dot{x}_j^2(t)}{2B_j}$ represents degree of aggressiveness that driver i desires to be. For example, when the two vehicles travel at the same speed, this term becomes $\gamma_i\dot{x}_i^2$ with:

$$\gamma_i = \frac{1}{2}(\frac{1}{b_i} - \frac{1}{B_j}) \tag{4}$$

where B_j represents driver i's estimate of the emergency deceleration which is most likely to be applied by driver j, while b_i can be interpreted as the deceleration *tolerable* by driver i. Attention should be drawn to the possibility that b_i might be greater than B_j in magnitude, which translates to the willingness (or aggressive characteristic) of driver i to take the risk of tailgating.

2.2 *Macroscopic model*

Under steady-state conditions, vehicles in the traffic behave uniformly and, thus, their identities can be dropped. Therefore, the microscopic LCM (Equations 3 and 4) can be aggregated to its macroscopic counterpart (traffic stream model):

$$v = v_f[1 - e^{1-\frac{k^*}{k}}] \tag{5}$$

where v is traffic space-mean speed, v_f free-flow speed, k traffic density, and k^* takes the following form:

$$k^* = \frac{1}{\gamma v^2 + \tau v + l} \tag{6}$$

where γ denotes the aggressiveness that characterizes the driving population, τ average response time that characterizes the driving population, and l average effective vehicle length. Equivalently, the macroscopic LCM can be expressed as:

$$k = \frac{1}{(\gamma v^2 + \tau v + l)[1 - \ln(1 - \frac{v}{v_f})]} \tag{7}$$

Note that an earlier version of LCM was proposed in [1], [2] which does not explicitly consider the effect of drivers' aggressiveness. To make a distinction, the LCM by default refers to the LCM formulated herein (both microscopic and macroscopic forms), whereas earlier version of the LCM will be referred to as the LCM without aggressiveness.

3 Model Properties

The LCM features a set of appealing properties that makes the model unique. First of all, it is a one-equation model that applies to a wide range of situations. More specifically, the microscopic LCM not only captures car-following regime, but also other regimes such as starting up, free-flow, approaching, cutting-off, stopping, etc., see [3] for more details. The macroscopic LCM applies to the entire range of density and speed without the need to identify break points.

Secondly, the LCM makes physical sense since it is rooted in basic principles (such as field theory and Newton's second law of motion). In addition, LCM employs a set of model parameters that are not only physical meaningful but also easy to calibrate. For example, the microscopic LCM involves desired speed v_i, perception-reaction time τ_i, desired maximum acceleration when starting from standing still A_i, tolerable deceleration b_i, emergency deceleration B_j, and effective vehicle length l_j. The macroscopic LCM includes aggregated parameters of free flow speed v_f, aggressiveness γ, average response time τ, and effective vehicle length l. Data to calibrate the above parameters are either readily available in publications (such as Motor Trend and human factors study reports) or can be sampled in the field with reasonable efforts.

Lastly, LCM models represent a consistent modeling approach, i.e., the macroscopic LCM is derived from its microscopic counter-part when aggregated over vehicles and time. Such micro-macro consistency not only supplies macroscopic modeling with a microscopic basis but also ensures that microscopic modeling aggregates to a predictable macroscopic behavior.

More properties are discussed in the following subsections.

3.1 Boundary conditions

The macroscopic LCM has two clearly defined boundary conditions. When density approaches zero ($k \to 0$), traffic speed approaches free-flow speed ($v \to v_f$); when density approaches jam density ($k \to k_j = 1/l$), traffic speed approaches zero ($v \to 0$), see Figure 9 in a later example for an instance.

Kinematic wave speed at jam density ω_j can be determined by finding the first derivative of flow q with respect to density k and evaluating the result at $k = k_j$. Hence,

$$q = kv = \frac{v}{(\gamma v^2 + \tau v + l)[1 - \ln(1 - \frac{v}{v_f})]} \tag{8}$$

After some math,

$$\frac{dq}{dk} = v + k\frac{dv}{dk} = v - \frac{(\gamma v^2 + \tau v + l)[1 - ln(1 - \frac{v}{v_f})]}{(2\gamma v + \tau)[1 - ln(1 - \frac{v}{v_f})] + (\gamma v^2 + \tau v + l)[\frac{1}{v_f - v}]} \tag{9}$$

Therefore, ω_j can be evaluated as:

$$\omega_j = \frac{dq}{dk}|_{k=k_j, v=0} = -\frac{l}{\tau + \frac{l}{v_f}} \tag{10}$$

Meanwhile, capacity q_m can be found by first setting Equation 9 to zero to solve for optimal speed v_m or optimal density k_m and then plugging v_m or k_m into Equation 8 to calculate q_m. However, it appears that an analytical solution of (q_m, k_m, v_m) is not easy to find and this is a limitation of the LCM. Fortunately, the problem can be easily addressed numerically.

On another note, the spacing-speed relationship is:

$$s = (\gamma v^2 + \tau v + l)[1 - ln(1 - \frac{v}{v_f})] \tag{11}$$

The slope of the speed-spacing relationship when traffic is jammed can be determined by finding the first derivative of $v = f(s)$ with respect to spacing s and evaluate the result at $s = l$ and $v = 0$:

$$\frac{dv}{ds}|_{s=l,v=0} = \frac{1}{(2\gamma v + \tau)[1 - ln(1 - \frac{v}{v_f})] + (\gamma v^2 + \tau v + l)[\frac{1}{v_f - v}]}|_{s=l,v=0} = \frac{1}{\tau + \frac{l}{v_f}} \tag{12}$$

3.2 Model flexibility

The macroscopic LCM employs four parameters that supply the model with sufficient flexibility to fit data from a wide range of facilities, as detailed in the next section. As originally noted by [4] and later by [5] and [6] that concavity is a desirable property of flow-density relationship. This property is empirically evident in field observations from most highway facilities, especially in outer lanes, and the shape of flow-density relationship looks like a parabola with varying skewness. In addition, some researchers [7, 8, 5, 6] recognize the attractiveness of having a triangular flow-density relationship. Moreover, a reverse-lambda shape was reported by [9, 10], most likely in the inner lane of freeway facilities. Therefore, a desirable property of a traffic stream model is its flexibility to represent a variety of flow-density shapes ranging from skewed parabola to triangular to reverse-lambda.

Figure 2 illustrates a family of fundamental diagrams generated from the macroscopic LCM with the following parameters: $v_f = 30$ m/s, $k_j = 1/5$ veh/m, $\tau = 1$ s, and aggressiveness γ ranging from 0 to -0.03 s^2/m. In the flow-density subplot, the lowest curve exhibiting a skewed parabolic shape is generated using $\gamma = 0$, the second highest curve showing nearly a triangular shape is generated using $\gamma = -0.027$, and the highest curve, which takes a reverse-lambda shape, is generated using $\gamma = -0.03$. From the definition of aggressiveness in Equation 4, one recognizes that smaller values of γ correspond to more aggressive drivers who are willing to accept shorter car-following distances. Therefore, the values of γ, the shape of $q - k$ curves, and field observations are consistent. Further quantitative analysis of the effect of aggressiveness and its interaction with other model parameters warrants further research and is not discussed here.

4 Empirical Results

Initial test results of the LCM at both microscopic and macroscopic levels without the consideration of driver aggressiveness were reported in [3]. Hence, this paper focuses on testing the LCM with consideration of aggressiveness by fitting the model to traffic flow data collected from a variety of facilities at different locations including Atlanta (US), Orlando (US), Germany, CA/PeMs (US), Toronto (Canada), and Amsterdam (Netherlands). Note that the fit of the LCM and other traffic stream models is conducted with careful efforts, but no optimal fitting is guaranteed.

Figures 3 through 8 illustrate field data observed at these facilities with data “clouds” in the background labeled as “Empirical”. Since the clouds are scattered to varying degrees, they are aggregated and the resultant data are shown as the “dots” labeled as “Emp mean”. The fit result of the LCM is illustrated as solid lines labeled as “LCM”. Also shown are the fit results of other traffic stream models including Underwood model [11] (which employs two parameters) and Newell model [12] (three parameters). As such, the reader is able to visually compare goodness-of-fit of two-, three-, and four-parameter models and examine how fit quality varies with number of parameters. Consisting of four subplots (namely, speed vs density, speed vs flow, flow vs density, and speed vs spacing), each figure illustrates the fundamental diagrams represented by empirical data and these models.

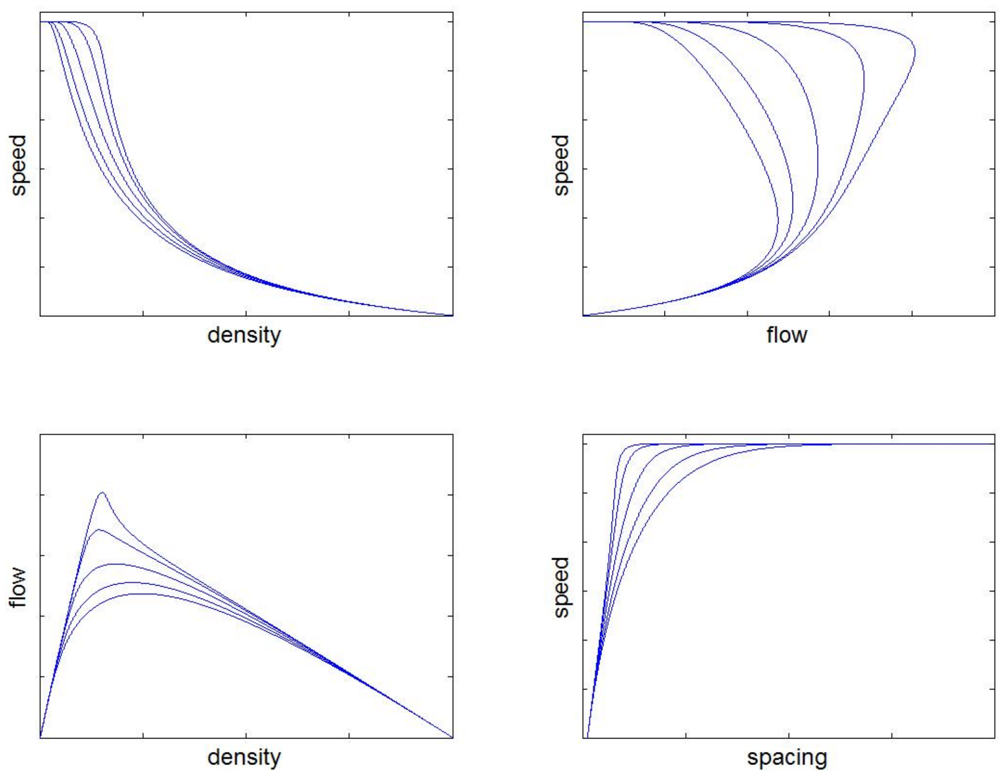

Figure 2: Family of curves generated from LCM with varying aggressiveness

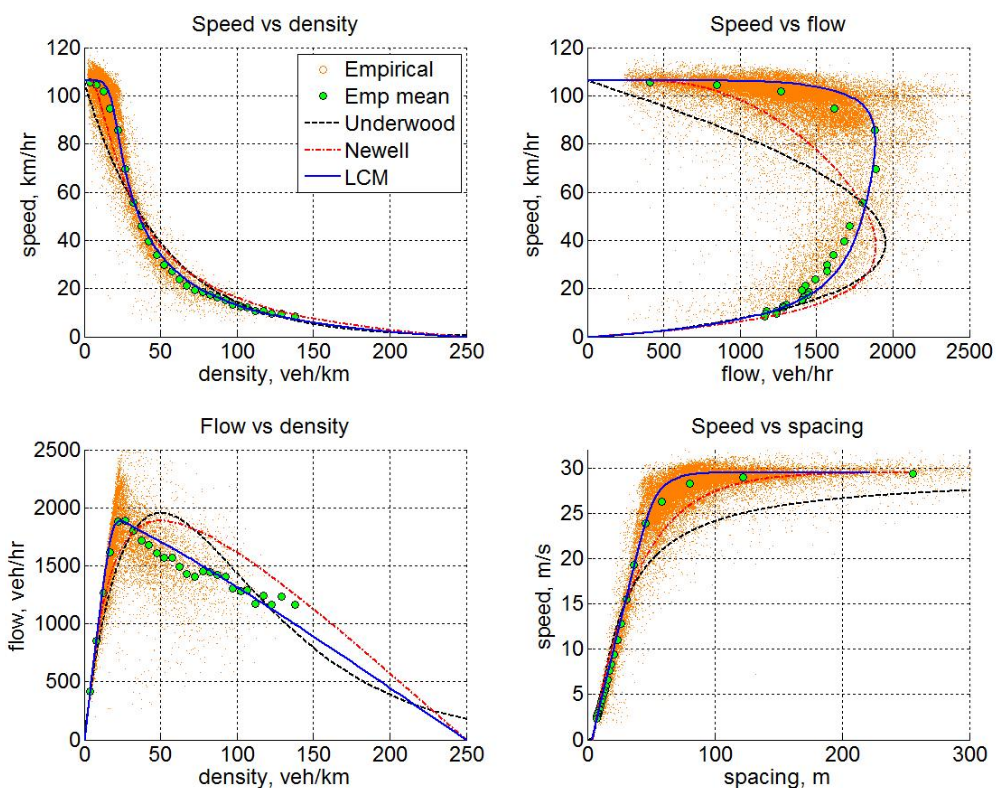

Figure 3: LCM fitted to GA400 Data

The empirical data in Figure 3 are collected on GA400, a toll road in Atlanta, GA, at station 4001116. Consisting of 4787 observation points, the abundant field data reveal the relationships among flow, density, and speed by means of cloud density, i.e. the intensity of data points. Meanwhile, the wide scatter of data points seems to suggest that any deterministic, functional fit is merely a rough approximation and a stochastic approach such as [13] might be more statistically sound. Combining the cloud and the large dots (i.e., Emp mean), one is able to identify the trend of the these relationships. For example, the flow-density relationship appears to be a reverse-lambda shape (if one looks at the cloud) or a triangle (if one looks at the large dots). Meanwhile, the speed-flow relationship features a $\supset$ shape with its "nose" tilting upward. After much trial-and-error effort, its seems that a reverse-lambda fit of flow-density relationship is not as good as a (nearly) triangular fit in terms of minimizing overall fitting error. As indicated in Table 1, the free-flow speed v_f is estimated as 106.2 km/h (29.5 m/s), effective vehicle length l = 4 m (or jam density k_j = 250 veh/km), average response time τ = 1.46 s, and aggressiveness γ = -0.038 s^2/m. Note that the effective vehicle length l is so estimated merely to yield a good fit. It is recognized that the value itself may appear somewhat small and there are actually no data points to support such a short effective vehicle length or equivalently high jam density. Empirical capacity q_m determined based on the large dots is 1883.8 veh/hr at optimal density k_m of 22.0 veh/km and optimal speed v_m of 85.8 km/hr, while the capacity condition estimated from LCM is (q_m = 1886.0 veh/hr, k_m = 23.3 veh/km, v_m = 81.0 km/hr).

Two additional models are fitted to the data and the results are presented in Table 2. It is apparent that the more parameters a model employs, the more flexible the model becomes and hence the more potential to result in a good fit. In the speed vs flow subplot of Figure 3, Underwood and Newell models are comparable in the congested regime (i.e., the lower portion of the graph), while in the free-flow regime (i.e., the upper portion of the graph) Newell model outperforms Underwood model since Newell model is closer to the dense cloud. In contrast, the LCM (which employs four parameters) yields the best fit among the three, as indicated by the close approximation of the LCM curve to the empirical data. More specifically, the LCM runs through the dense cloud in the free-flow regime and follows the trend nicely in the rest of the graph. However, compared with the large dots (Emp mean), the LCM appears to over-estimate speed toward the end of the free-flow regime and under-estimate speed at the beginning of the congested regime. Nevertheless, whether such fitting errors are systematic has yet to be examined across empirical data from different locations. In the flow vs density subplot, both Underwood model and Newell model peak at about the same location ($k_m \approx$ 50 v/km). In the congested regime (i.e., the portion after the peak), both models exhibit a lack of fit with Newell model slightly better in terms of concavity while Underwood model slightly better in terms of closeness to data points. In contrast, the LCM is superior on all accounts. Not only does it exhibit the desirable shape (almost a triangle) but its proximity to empirical observations is much closer. In addition, the curve peaks at the same location where the empirical data peaks (k_m = 22 v/km). The speed vs density subplot does not reveal much information regarding the relative merit of these models since each appears to fit the empirical data nicely except for some slight differences here and there. The speed vs spacing subplot emphasizes the free-flow regime which is the flat portion in the top of the graph. It appears that Underwood model walks a long way to approach free-flow speed, while Newell model and the LCM adapt to free-flow speed sooner with a slight under- and over-fit respectively. Unfortunately, the congested regime (the slope at the beginning portion of this graph) does not reveal much difference among the three models since they all cluster tightly together.

As shown in Figure 4 and Table 1, I-4 data in Orlando, FL feature a capacity q_m of 1795.5 veh/hr which is achieved at an optimal density k_m of 22.1 veh/km and optimal speed v_m of 81.4 km/hr. What's striking in this set of data is that the free-flow regime in the speed vs flow subplot is almost flat and this condition sustains almost up to capacity. This graph clearly differentiates fit quality of models with different number of parameters. More specifically, the two-parameter Underwood model exhibits the least fit since its upper branch (i.e. free-flow regime), nose (i.e. capacity), and lower branch (i.e. congested regime) are far from empirical observations. The three-parameter Newell model is better as indicated by the closer fit of its upper branch, nose, and lower branch. The four-parameter LCM is superior in all aspects. For example, its upper branch is almost a flat line running through empirical data points, its nose tilts upward and roughly coincides with empirically observed capacity, and its lower branch cuts evenly through empirical observations. Though there are discrepancies between the empirical data and the fitted curve, no systematic over- or under-fit is observed in this graph. In the remaining three subplots, the differences among the three models and their fit quality are consistent with those observed in the speed vs flow subplot.

In Figure 5, the Autobahn data collected from Germany exhibit an unusually high free-flow speed v_f of 43.3 m/s (or 155.9 km/hr). Unlike the I-4 data which feature an almost constant free-flow speed v_f up to capacity, traffic speed in the Autobahn data gradually decreases in free-flow regime, resulting in an optimal speed v_m of only about 60% of v_f, as indicated in the speed vs flow subplot. Unfortunately, the particular nature of this set of data poses

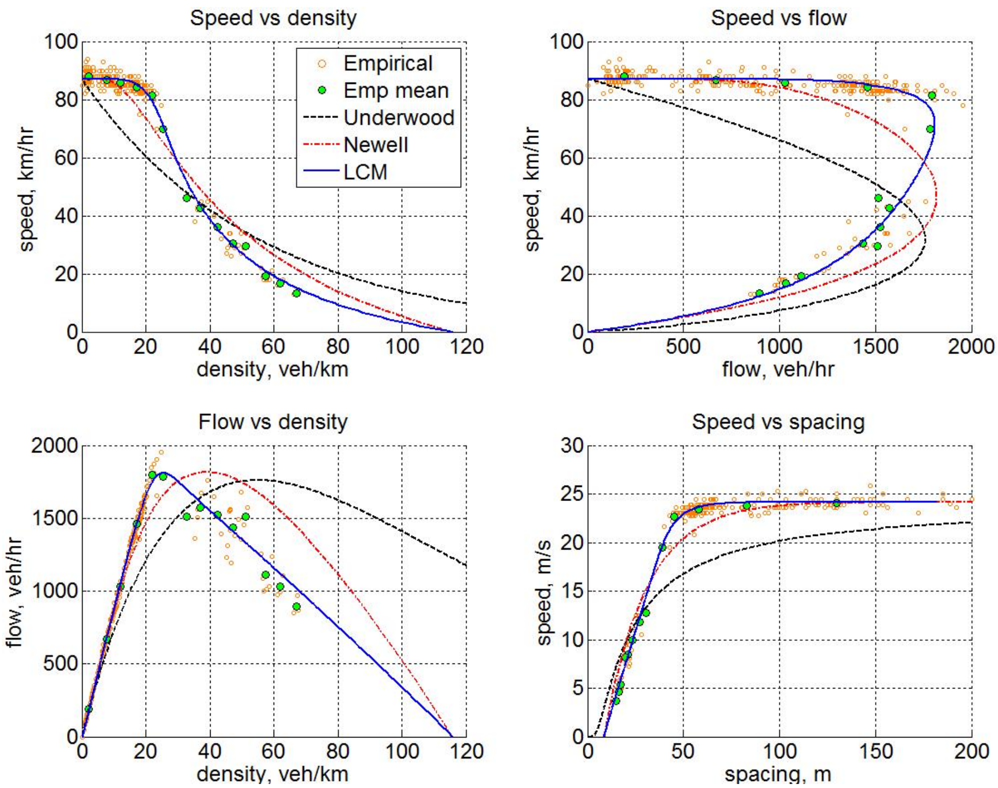

Figure 4: LCM fitted to I-4 Data

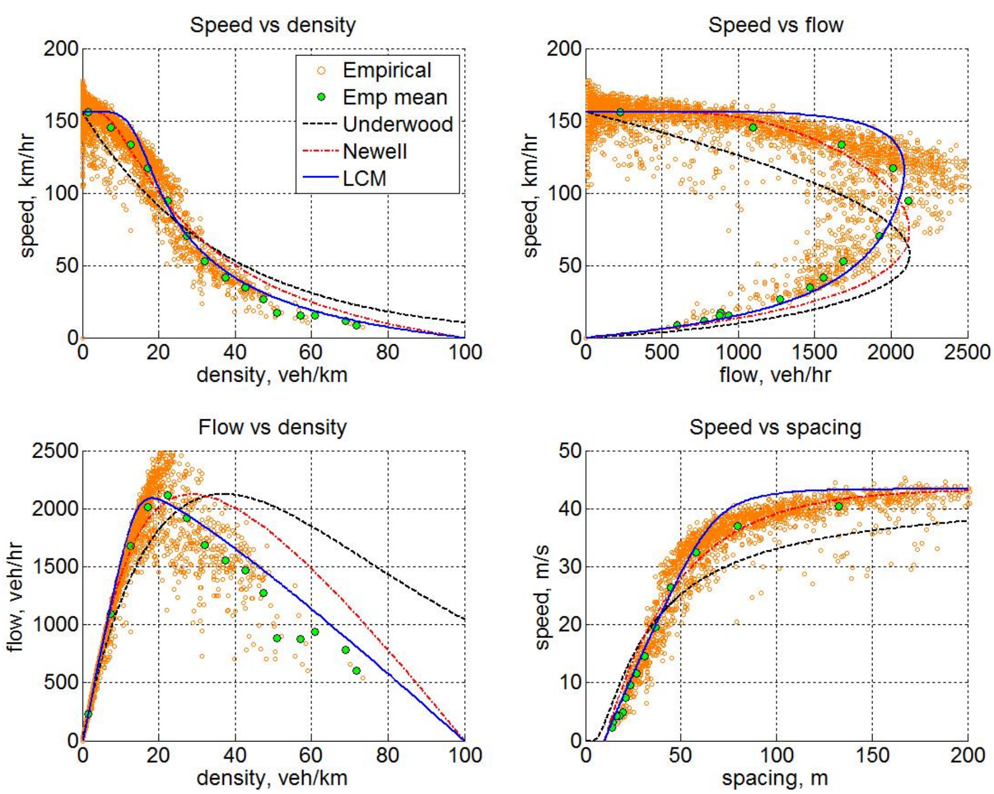

Figure 5: LCM fitted to Autobahn Data

a great challenge to any effort that attempts to fit the data. In the speed vs flow subplot, one has difficulty to fit a model that meets the observed free-flow regime, the congested regime, and the capacity simultaneously, so a trade-off has to be made among the three portions. The LCM curve shown has been tweaked between free-flow and congested regimes while guaranteeing the capacity. Though better than Underwood and Newell models, the LCM still exhibits some discrepancies compared with the empirical data.

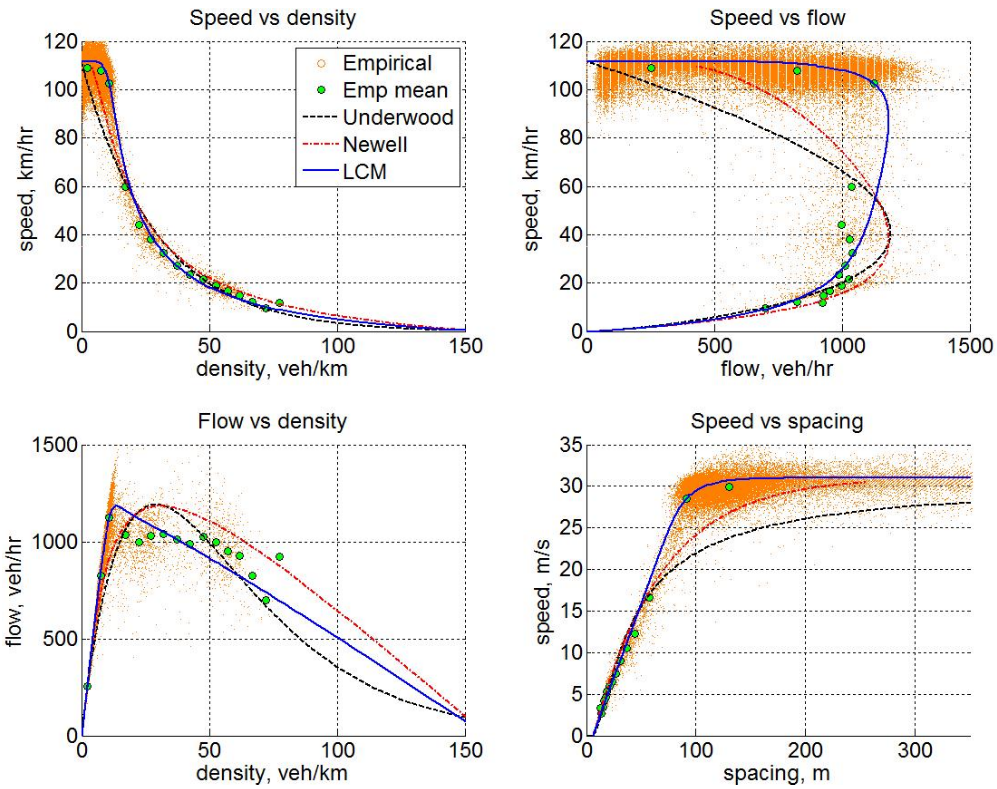

Figure 6: LCM fitted to PeMS Data

The PeMS data collected from California is plotted in Figure 6. This set of data heavily emphasizes the free-flow regime (which is virtually a flat band) with observations elsewhere sparsely scattered. Therefore, the fit of a model in regimes other than free flow might be arbitrary. With this understanding, LCM approximates the free-flow regime the best, while Underwood and Newell models are slanted and significantly underestimate optimal speed v_m.

Though field observation on Highway 401 in Toronto do not have abundant data points, a trends is still clearly established in each subplot of Figure 7. Much like the results in the I-4 data, there are clearly differences in capabilities among the models, with two-parameter Underwood model being the least and the four-parameter model the best. Notice that no systematic under- or over-fit is observed in the LCM curves.

The same comments as above apply to Ring Road data in Amsterdam, see Figure 8. In summary, estimated parameters of the LCM that result from fitting to various facility types are listed in Table 1 and cross-comparison of traffic stream models fitted to various facility types is listed in Table 2.

5 Applications

Since the LCM takes a simple mathematical form that involves physically meaningful parameters, the model can be easily applied to help investigate traffic phenomena at both microscopic and macroscopic levels. For illustration purpose, a concrete example is provided below, in which a moving bottleneck is created by a sluggish truck. Microscopic modeling allows the LCM to generate profiles of vehicle motion so that the cause and effect of vehicles slowing down or speeding up can be analyzed in exhaustive detail; macroscopic modeling may employ the LCM to generate fundamental diagrams that help determine shock paths and develop graphical solutions; Since the LCM is consistent at the

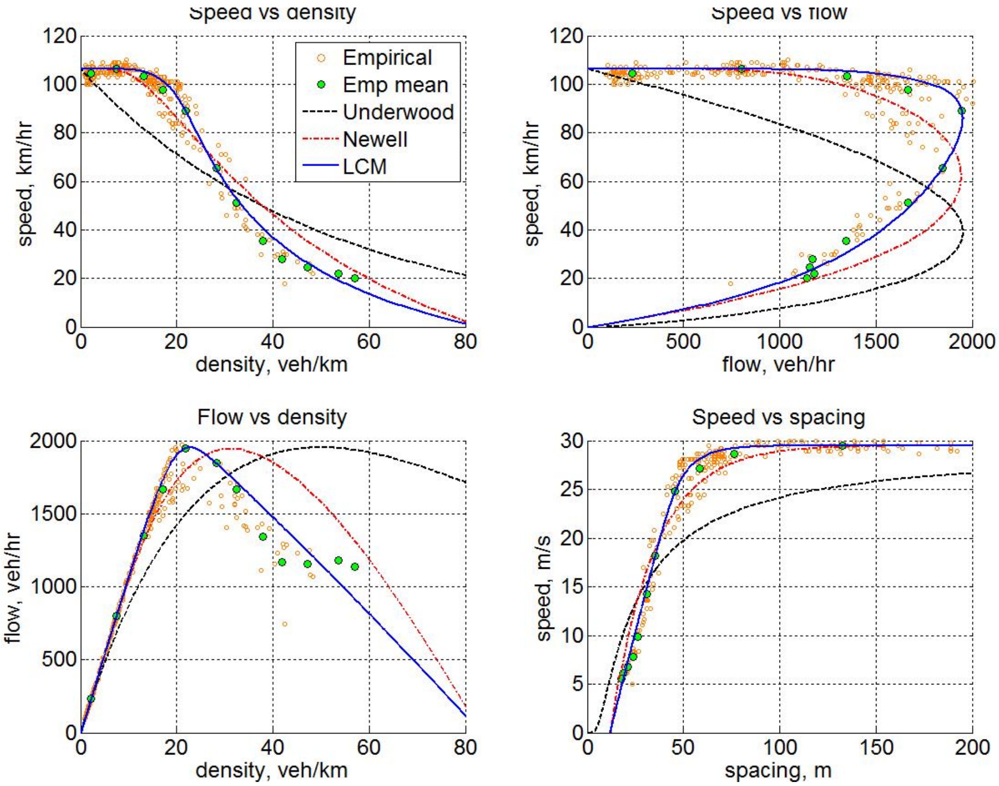

Figure 7: LCM fitted to Highway 401 Data

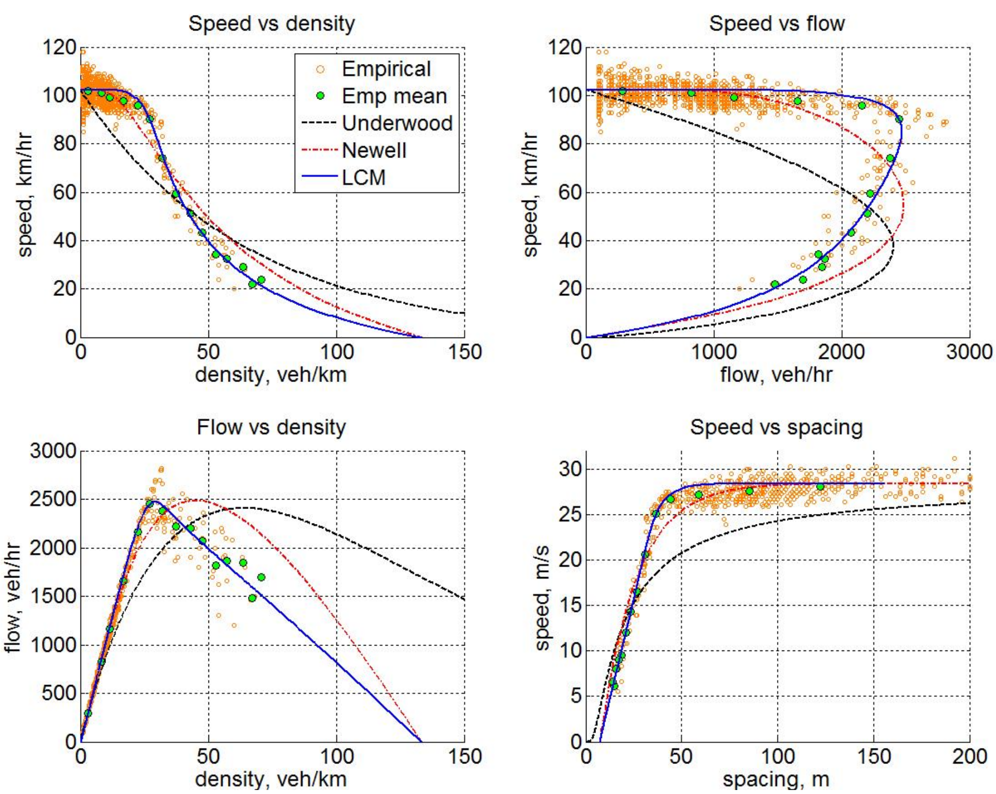

Figure 8: LCM fitted to Amsterdam Data

Table 1: Parameters of LCM as a result of fitting to various facility types

Data source			**Empirical parameters**				**Capacity condition**		
Location	Facility	No. obs.	v_f m/s	l m	τ s	γ s^2/m	q_m v/h	k_m v/km	v_m km/h
Atlanta	GA400	4787	29.5	4	1.46	-0.038	1883.8	22.0	85.8
Orlando	I-4	288	24.2	8.6	1.09	-0.040	1795.5	22.1	81.4
Germany	Autobahn	3405	43.3	10	1.0	-0.018	2114.1	22.3	95.0
CA/PeMs	Freeway	2576	31	6.3	2.4	-0.060	1124.9	11.0	102.5
Toronto	Hwy 401	286	29.5	12	0.8	-0.026	1945.7	21.8	89.2
Amsterdam	Ring Rd	1199	28.4	7.5	0.82	-0.026	2452.2	27.2	90.3

Table 2: Comparison of traffic stream models fitted to various facility types

Location	**Model**	**Estimated parameters**
Atlanta	Underwood	v_f = 29.5 m/s, k_m = 0.050 v/m
	Newell	v_f = 29.5 m/s, l = 4.0 m, λ = 0.81 1/s
	LCM	v_f = 29.5 m/s, l = 4.0 m, τ = 1.46 s, γ = -0.038 s^2/m;
Orlando	Underwood	v_f = 24.2 m/s, k_m = 0.055 v/m
	Newell	v_f = 24.2 m/s, l = 8.6 m, λ = 1.09 1/s
	LCM	v_f = 24.2 m/s, l = 8.6 m, τ = 1.09 s, γ = -0.040 s^2/m;
Germany	Underwood	v_f = 43.3 m/s, k_m = 0.037 v/m
	Newell	v_f = 43.3 m/s, l = 10.0 m, λ = 1.12 1/s
	LCM	v_f = 43.3 m/s, l = 10.0 m, τ = 1.00 s, γ = -0.018 s^2/m;
CA/PeMs	Underwood	v_f = 31.0 m/s, k_m = 0.029 v/m
	Newell	v_f = 31.0 m/s, l = 6.3 m, λ = 0.50 1/s
	LCM	v_f = 31.0 m/s, l = 6.3 m, τ = 2.40 s, γ = -0.060 s^2/m;
Toronto	Underwood	v_f = 29.5 m/s, k_m = 0.050 v/m
	Newell	v_f = 29.5 m/s, l = 12.0 m, λ = 1.3 1/s
	LCM	v_f = 29.5 m/s, l = 12.0 m, τ = 0.80 s, γ = -0.026 s^2/m;
Amsterdam	Underwood	v_f = 28.4 m/s, k_m = 0.064 v/m
	Newell	v_f = 28.4 m/s, l = 7.5 m, λ = 1.5 1/s
	LCM	v_f = 28.4 m/s, l = 7.5 m, τ = 0.82 s, γ = -0.026 s^2/m;

microscopic and macroscopic levels, the two sets of solutions not only agree with but also complement each other.

In addition, the LCM can be adopted by existing commercial simulation packages to improve their internal logic of car following, or it can serve as the basis of a new simulation package. Moreover, the LCM can be adopted in highway capacity and level of service (LOS) analysis. For example, conventional LOS analysis procedure involves the use of speed-flow curves to determine traffic speed, see [14] for the family of curves in EXHIBIT 23-3 and the set of approximating equations underneath. The macroscopic LCM can help make the analysis more effectively by providing more realistic speed-density curves to facilitate analytical, numerical, and graphical solutions. Furthermore, the LCM can be adopted by transportation planners to be used as the basis of a highway performance function which realistically estimates travel time (via traffic speed) as a function of traffic flow assigned to a route. The resultant travel time is the basis of driver route choice behavior, which in turn stipulates dynamic traffic assignment.

5.1 An illustrative example

A freeway segment contains an on-ramp (which is located at 2000 m away from an arbitrary reference point denoting the upstream end of the freeway) followed by an off-ramp 2000 m apart. The freeway was initially operating under condition A (flow 0.3333 veh/s or 1200 veh/hr, density 0.1111 veh/m or 17.9 veh/mi, and speed 30 m/s or 67.1 mi/hr). At 2:30pm, a slow truck enters the freeway traveling at a speed of 5.56 m/s which forces the traffic to operate under condition B (flow 0.3782 veh/s or 1361 veh/hr, density 0.0681 veh/m or 109.6 veh/mi, and speed 5.56 m/s or 12.4 mi/hr). After a while, the truck turns off the freeway at the next exit. The impact on the traffic due to the slow truck is illustrated macroscopically in subsection 5.2 and microscopically in subsections 5.3 and 5.4.

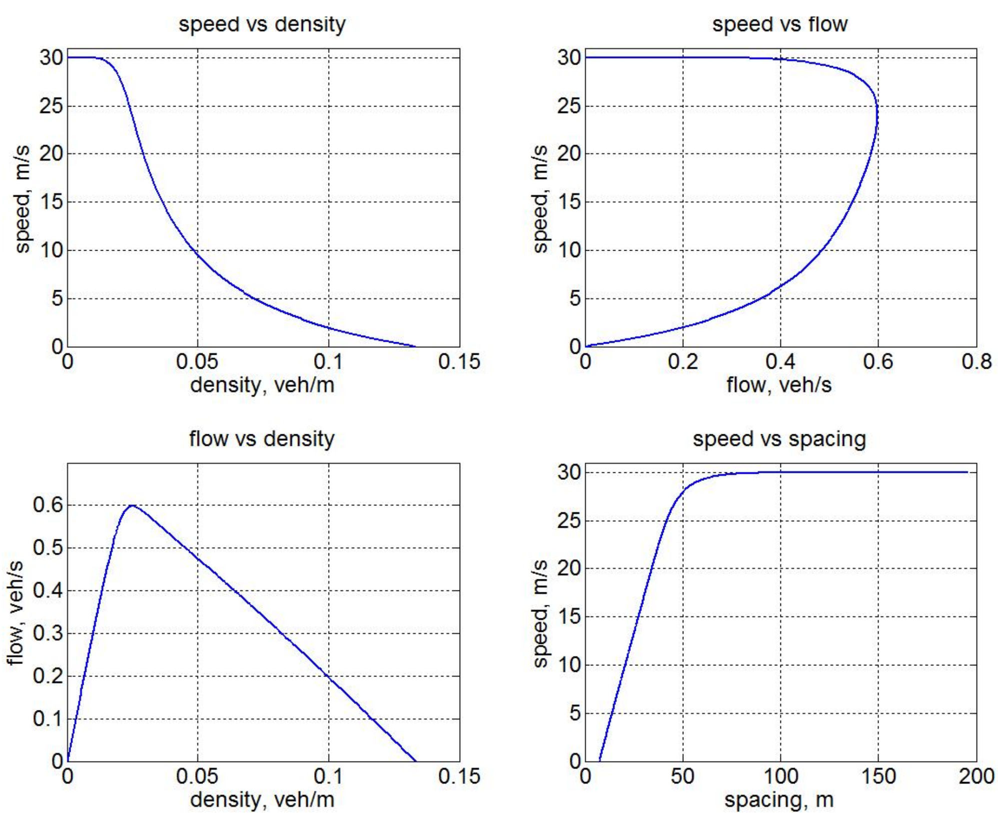

Figure 9: Fundamental diagram of the freeway generated from LCM

A fundamental diagram, which is illustrated in Figure 9, is generated using the macroscopic LCM to characterize the freeway with the following parameters: free-flow speed $v_f = 30$ m/s, aggressiveness $\gamma = -0.028$ m/s^2, average response time $\tau = 1$ second, and effective vehicle length $l = 7.5$ m. In addition, the above-mentioned traffic flow conditions, free-flow condition O, and capacity condition C are tabulated in Table 3.

To illustrate the application of the LCM, the above problem is addressed in two approaches: macroscopic

Table 3: Traffic flow conditions

Condition	Flow, q veh/s (veh/hr)	Density k veh/m (veh/mi)	Speed v m/s (mi/hr)
A	0.3333 (1200.0)	0.0111 (17.9)	30 (67.1)
B	0.3782 (1361.6)	0.0681 (109.6)	5.56 (12.4)
C	0.5983 (2154.0)	0.0249 (40.1)	24.03 (53.7)
O	0 (0)	0 (0)	30 (67.1)

graphical solution and microscopic simulation solution. The microscopic simulation is conducted in deterministic and random fashions.

5.2 *Macroscopic approach - graphical solution*

The graphical solution to the problem involves finding shock paths that delineate time-space (t-x) regions of different traffic conditions. Figure 10 illustrates the time-space plane overlaid with the freeway on the right and a mini-version of the flow-density plot in the top-left corner. The point when the slow truck enters the freeway (2:30pm) roughly corresponds to $P_1(t_1 = 65, x_1 = 2000)$ on the time-space plane, while the point when the truck turns off the freeway is roughly $P_3(t_3 = 425, x_3 = 4000)$. Therefore, constrained by the truck, the t-x region under P_1P_3 should contain traffic condition B. On the other hand, the t-x regions before the truck enters and before congestion (i.e. condition B) forms should have condition A. As such, there must be a shock path that delineates the two regions, and such a path should start at P_1 with a slope equal to shock wave speed U_{AB} which can be determined according to Rankine-Hugonoit jump condition [15] [16]:

$$U_{AB} = \frac{q_B - q_A}{k_B - k_A} = \frac{0.3782 - 0.3333}{0.0681 - 0.0111} = 0.7877\text{m/s} \tag{13}$$

Meanwhile, at downstream of the off-ramp, congested traffic departs at capacity condition C, which corresponds to a t-x region that starts at P_3 and extends forward in time and space. Hence, a shock path forms between the region with condition C and the region with condition B. Such a shock path starts at P_3 and runs at a slope equal to shock wave speed U_{BC}:

$$U_{BC} = \frac{q_C - q_B}{k_C - k_B} = \frac{0.5983 - 0.3782}{0.0249 - 0.0681} = -5.0949\text{m/s} \tag{14}$$

If the flow-density plot is properly scaled, one should be able to construct the above shock paths on the t-x plane. The two shock paths should eventually meet at point $P_2(t_2, x_2)$ whose location can be found by solving the following set of equations:

$$\begin{cases} x_2 - x_1 & = U_{AB} \times (t_2 - t_1) \\ x_2 - x_3 & = U_{BC} \times (t_2 - t_3) \\ (x_2 - x_1) + (x_3 - x_2) & = 2000 \end{cases} \tag{15}$$

After some math, P_2 is determined roughly at $(716.8, 2513.4)$. After the two shock paths P_1P_2 and P_3P_2 meet, they both terminate and a new shock path forms which delineates regions with conditions C and A. The slope of the shock path should be equal to shock speed U_{AC}:

$$U_{AC} = \frac{q_C - q_A}{k_C - k_A} = \frac{0.5983 - 0.3333}{0.0249 - 0.0111} = 19.2029\text{m/s} \tag{16}$$

As such, the shock path can be constructed as P_2P_4. Lastly, the blank area in the t-x plane denotes a region with no traffic, i.e. condition O.

5.3 Microscopic approach - deterministic simulation

In order to double check on the LCM and to verify if its macroscopic and macroscopic solutions agree with each other reasonably, the microscopic LCM is implemented in Matlab, a computational software package. As a manageable starting point, the microscopic simulation is made deterministic with the following parameters: desired speed $v_i = 30$ m/s, maximum acceleration $A_i = 4$ m/s^2, emergency deceleration $B_i = 6$ m/s^2, tolerable deceleration $b_i = 9$ m/s^2, perception-reaction time $\tau_i = 1$ second, and effective vehicle length $l_i = 7.5$ m, where $i \in \{1, 2, 3, ..., n\}$ are unique vehicle identifiers. Vehicles arrive at the upstream end of the freeway at a rate of one vehicle every three seconds, which corresponds to a flow of $q = 1200$ veh/hr. Simulation time increment is one second and simulation duration is 1000 seconds.

Figure 10 illustrates the simulation result in which vehicle trajectories are plotted on the t-x plane. The varying density of trajectories outlines a few regions with clearly visible boundaries. The motion or trajectory of the first vehicle is pre-determined, while those of the remaining vehicles are determined by the LCM. The first vehicle enters the freeway at time $t = 65$ seconds after the simulation starts. This moment is calculated so that the second vehicle is about to arrive at the on-ramp at this particular moment. Hence, the second vehicle and vehicles thereafter have to adopt the speed of the truck, forming a congested region where traffic operates at condition B.

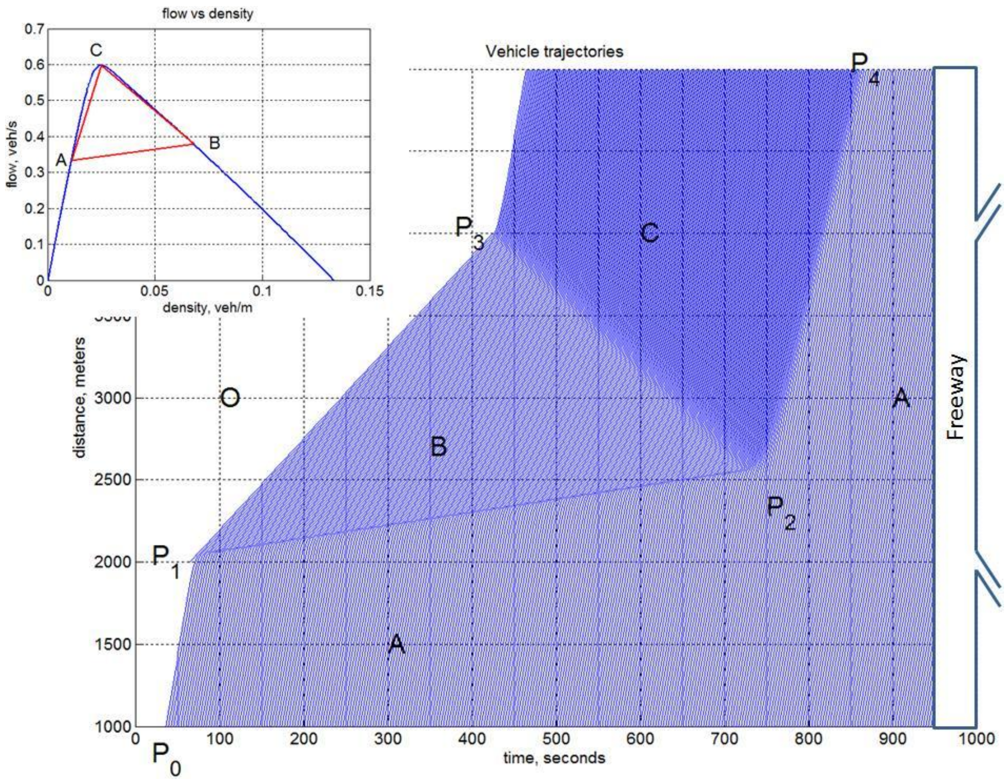

Figure 10: A moving bottleneck due to a slow truck, deterministic simulation

Upstream of this congested region B is a region where traffic arrives according to condition A. The interface of regions B and A, P_1P_2, denotes a shock path in which vehicles in fast platoon A catch up with and join slow platoon B ahead. The situation continues and the queue keeps growing till the truck turns off the freeway at $t = 425$ second into the simulation. After that, vehicles at the head of the queue begin to accelerate according to the LCM, i.e. traffic begins to discharge at capacity condition C. Therefore, the front of the queue shrinks, leaving a shock path P_3P_2 that separates region C from region B. Since the queue front shrinks faster than the growth of queue tail, the former eventually catches up with the later at P_2, at which point both shock paths terminate denoting end of congestion. After the congestion disappears, the impact of the slow truck still remains because it leaves a capacity flow C in front followed by a lighter and faster flow with condition A. Hence the trace where faster vehicles in platoon A join platoon C denotes a new shock path P_2P_4.

Comparison of the macroscopic graphical solution and the microscopic deterministic simulation reveals that they agree with each other very well, though the microscopic simulation contains much more information about the motion of each individual vehicle and the temporal-spatial formation and dissipation of congestion.

5.4 Microscopic approach - random simulation

Since the microscopic approach allows the luxury to account for randomness in drivers and traffic flow, the following simulation may replicate the originally posed problem more realistically. The randomness of the above example is set up as follows with the choice of distribution forms being rather arbitrary provided that they are convenient and reasonable:

- Traffic arrival follows Poisson distribution, in which the headway between the arrival of consecutive vehicles is exponentially distributed with mean 3 seconds, i.e. $h_i \sim$ Exponential$(3)s$, which corresponds to a flow of 1200 veh/hr;
- Desired speed follows a normal distribution: $v_i \sim N(30, 2)$ m/s;
- Maximum acceleration follows a triangular distribution: $A_i \sim$ Triangular$(3, 5, 4)$ m/s^2;
- Emergency deceleration: $B_i \sim$ Triangular$(5, 7, 6)$ m/s^2;
- Tolerable deceleration: $b_i \sim$ Triangular$(8, 10, 9)$ m/s^2;
- Effective vehicle length: $l_i \sim$ Triangular$(5.5, 9.5, 7.5)$ m;

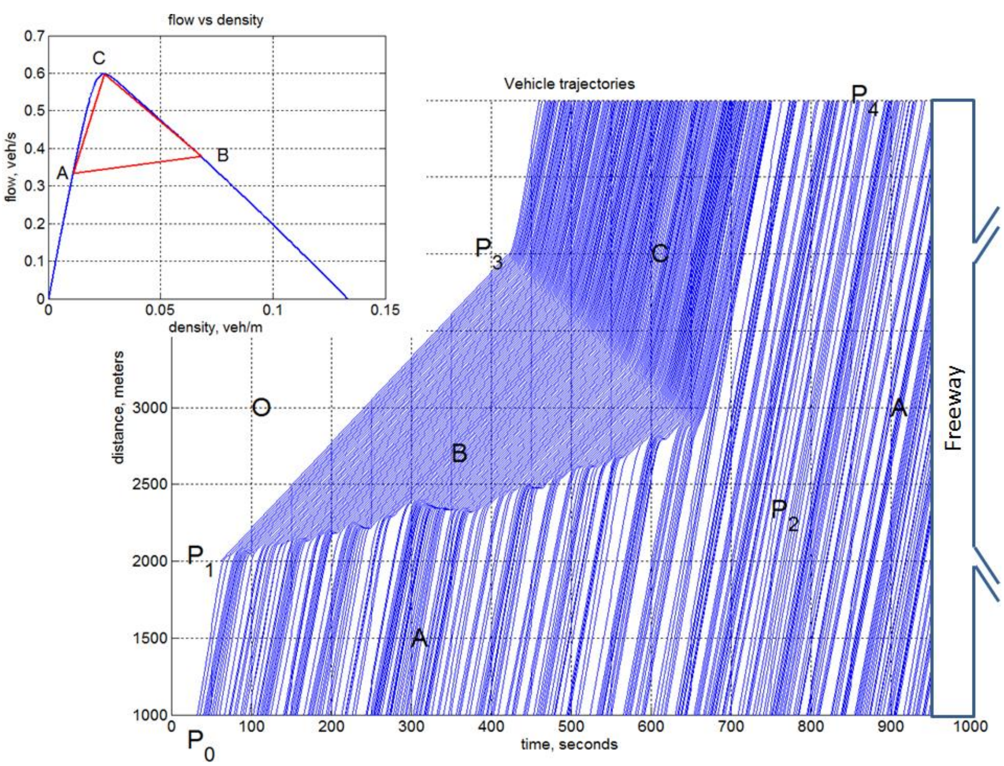

Figure 11: A moving bottleneck due to a slow truck, random simulation

The result of one random simulation run is illustrated in Figure 11 where the effect of randomness is clearly observable. Trajectories in region B seem to exhibit the least randomness because vehicles tend to behave uniformly under congestion. Trajectories in region C are somewhat random since the metering effect due to the congestion still remains. In contrast, region A appears to have the most randomness not only because of the Poisson arrival pattern but also the random characteristics of drivers. Consequently, the shock path between regions B and C, P_3P_2 remains almost unaltered, while there is much change in shock path P_1P_2. The first is the roughness of the shock path and this is because now vehicles in platoon A joins the tail of the queue in a random fashion. The second is that the path might not be a straight line. As a matter of fact, the beginning part of the shock path has a slope roughly equal to U_{AB}, while the rest part has a slightly steeper slope (due to less intense arrival from upstream during this period) resulting in the termination of congestion earlier than the deterministic case (which is somewhere near P_2). This, in turn, causes the slope of the shock path between regions C and A to shift left. Note that the slope of this shock path remains nearly the same since this scenario features a fast platoon being caught up with by an even faster platoon.

6 Related Work

The microscopic LCM is a dynamic model which stipulates the desired motion (or acceleration) of a vehicle as the result of the overall field perceived by the driver. Other examples of dynamic model are GM models [17, 18] and the Intelligent Driver Model (IDM) [19, 20]. A dynamic model may reduce to a steady-state model when vehicle acceleration becomes zero. A steady-state model essentially represents a safety rule, i.e., the driver's choice of speed as a result of car-following distance or vice versa. Examples of steady-state models include Pipes model [21], Forbes model [22, 23, 24], Newell nonlinear car-following model [12], Gipps car-following model [25], and Van Aerde car-following model [26, 27]. Interested readers are referred to [28] for a detailed discussion on the relation among LCM and other car-following models including a unified diagram that summarizes such relation.

The microscopic LCM incorporates a term called desired spacing s^*_{ij} (Equation 2) which generally admits any safety rule and consequently any steady-state model. However, Equation 3 instantiates s^*_{ij} in a quadratic form as a simplified version of Gipps car-following model [25]. The result coincides with the speed-spacing relation documented in Highway Capacity Manual [29] and Chapter 4 of [30] as a result of 23 observational studies. The speed-spacing relation incorporates three terms: a constant term representing effective vehicle length, a first order term which is the distance traveled during perception-reaction time τ, and a second order term, which is the difference of the breaking distances by the following and leading vehicles, is interpreted in this paper as the degree of aggressiveness that the following driver desires to be. If one ignores the second order term, Pipes model [21] and equivalently Forbes model [22, 23, 24] are resulted.

The macroscopic model is a single-regime traffic stream (or equilibrium) model involving four parameters. Also in the single-regime category, Van Aerde model [26, 27] and IDM [19, 20] involve four parameters, Newell model [12] and Del Castillo models [5, 31] have three parameters, and early traffic stream models such as [32], [33], [11], and [34] models necessitate only two parameters, though their flexibility and quality of fitting vary as illustrated in Section 4.

7 Conclusions

This paper proposed a simple yet efficient traffic flow model, the longitudinal control model (LCM), which is a result of modeling from a combined perspective of Physics and Human Factors. The LCM model is formulated in two consistent forms: the microscopic model describes vehicle longitudinal operational control and the macroscopic model characterizes steady-state traffic flow behavior and further the fundamental diagram.

The LCM model is tested by fitting to empirical data collected at a variety of facility types in different locations including GA400 in Atlanta, I-4 in Orlando (US), Autobahn in Germany, PeMs in California, Highway 401 in Toronto, and Ring Road in Amsterdam. The wide scatter of these data sets suggest that any deterministic, functional fit is merely a rough approximation and a stochastic approach might be more statistically sound. Test results support the claim that the LCM has sufficient flexibility to yield quality fits to these data sets. Meanwhile, two more models are fitted to the same data sets in order to establish perspective on the LCM. These models include the two-parameter Underwood model and the three-parameter Newell model. Fit results reveal that the more parameters a model employs, the more flexible the model becomes and hence the more potential to result in a good fit. Consistently, Underwood model yields the least goodness-of-fit, while Newell model represents an upgrade and the LCM maintains the best fit to empirical data.

The unique set of properties possessed by the LCM lend itself to various transportation applications. For example, the LCM can be easily applied to help investigate traffic phenomena. An illustrative example is provided showing how to apply the LCM to analyze the impact of a sluggish truck at both microscopic and macroscopic levels.

Noticeably, the two sets of solutions agree with and complement each other due to the consistency of the LCM. In addition, the LCM can be adopted by existing commercial simulation packages to improve their internal logic of car following, or perhaps serves as the basis of a new simulation package. Moreover, the LCM may help make highway capacity and level of service (LOS) analysis more effectively by providing more realistic speed-density curves to facilitate analytical, numerical, and graphical solutions. Further more, the LCM can assist effective transportation planning by providing a better highway performance function that helps determine driver route choice behavior.

Acknowledgement

This research was partially supported by University Transportation Center program.

References

[1] Daiheng Ni. Multiscale Modeling of Traffic Flow. *Mathematica Aeterna, Hilaris Ltd.*, 1(01):27–54, 2011.

[2] Daiheng Ni. A Unified Perspective on Traffic Flow Theory, Part I: The Field Theory. In *The proceedings of ASCE-ICCTP 2011 (Paper# 30)*, Nanjing, China, 2011. American Society of Civil Engineers.

[3] Daiheng Ni, Cheng Zhang, and Haizhong Wang. A Unified Perspective on Traffic Flow Theory, Part III: Validation and Benchmarking. In *The proceedings of ASCE-ICCTP 2011 (Paper# 32)*, Nanjing, China, 2011. American Society of Civil Engineers.

[4] G.B. Whitham. *Linear and Nonlinear Waves*. John Wileyand Sons Inc, New York, NY., 1974.

[5] J. M. Del Castillo and F. G. Bentez. On the Functional Form of the Speed-Density Relationship - I: General Theory. *Transportation Research Part B: Methodological*, 29(5):373–389, 1995.

[6] Hesham Rakha. Validation of Van Aerde's Simplified Steadystate Car-Following and Traffic Stream Model. *Transportation Letters. International Journal of Transportation Research*, 1(3):227–244, 2009.

[7] G.F. Newell. A Simplified Theory on Kinematic Waves in Highway Traffic, Part II: Queueing at Freeway Bottlenecks. *Transportation Research B*, 27(4):289–303, 1993.

[8] C.F. Daganzo. The Cell Transmission Model: A Dynamic Representation of Highway Traffic Consistent with the Hydrodynamic Theory. *Transportation Research B*, 28(4):269–287, 1994.

[9] M. Koshi, M. Iwasaki, and I. Ohkura. Some Findings and an Overview on Vehicular Flow Characteristics. In *8th International Symposium on Transportation and Traffic Flow Theory*, pages 403–426, Toronto, 1983.

[10] J. H. Banks. Freeway Speed-Flow-Concentration Relationships: More Evidence and Interpretations. *Transportation Research Record*, 1225:53–60, 1989.

[11] R.T. Underwood. Speed, Volume and Density Relationships. *Quality and Theory of Traffic Flow, Yale University Report, New Haven, Connecticut*, 1961.

[12] G. F. Newell. Nonlinear Effects in the Dynamics of Car Following. *Operations Research*, 9(2):209–229, 1961.

[13] Haizhong Wang, Daiheng Ni, Qian-Yong Chen, and Jia Li. Stochastic Modeling of Equilibrium Speed-Density Relationship. *To appear in Journal of Advanced Transportation (DOI: 10.1002/atr.172), John Wiley & Sons, Inc.*, 2011.

[14] *Highway Capacity Manual*. Transportation Research Board, 2000.

[15] W. J. M. Rankine. On the Thermodynamic Theory of Waves of Finite Longitudinal Disturbances. *Philosophical Transactions of the Royal Society*, 160:277–288, 1870.

[16] H. Hugoniot. Propagation des Mouvements dans les Corps et spcialement dans les Gaz Parfaits" (in French). *Journal de l'Ecole Polytechnique*, 57:3, 1887.

[17] R.E. Chandler, R. Herman, and E.W. Montroll. Traffic Dynamics: Studies in Car Following. *Operations Research*, 6:165–184, 1958.

[18] D. C. Gazis, R. Herman, and R. W. Rothery. Non-Linear Follow the Leader Models of Traffic Flow. *Operations Research*, 9:545–567, 1961.

[19] Martin Treiber, Ansgar Hennecke, , and Dirk Helbing. Congested Traffic States in Empirical Observations and Microscopic Simulations. *Phys. Rev. E*, 62:18051824, 2000.

[20] D. Helbing, A. Hennecke, V. Shvetsov, and M. Treiber. Micro- and Macro-Simulation of Freeway Traffic. *Mathematical and Computer Modelling*, 35(5):517–547, 2002.

[21] L. A Pipes. An Operational Analysis of Traffic Dynamics. *Journal of Applied Physics*, 24:271–281, 1953.

[22] T.W. Forbes, H.J. Zagorski, E.L. Holshouser, and W A. Deterline. Measurement of Driver Reaction to Tunnel Conditions. *Proceedings of Highway Research Board*, 37:345–357, 1958.

[23] T.W. Forbes. Human Factor Considerations in Traffic Flow Theory. *Highway Research Record*, 15:60–66, 1963.

[24] T. Forbes and M. Simpson. Driver and Vehicle Response in Freeway Deceleration Waves. *Transportation Science*, 2(1):77–104, 1968.

[25] P.G. Gipps. A Behavioral Car Following Model for Computer Simulation. *Transportation Research, Part B*, 15:105–111, 1981.

[26] M. Van Aerde. Single Regime Speed-Flow-Density Relationship for Congested and Uncongested Highways. In *Presented at the 74th Transportation Research Board (TRB) Annual Meeting, Paper number 950802*, Washington, D.C., 1995.

[27] M. Van Aerde and H. Rakha. Multivariate Calibration of Single Regime Speed-Flow-Density Relationships. In *Proceedings of the 6th 1995 Vehicle Navigation and Information Systems Conference*, pages 334–341, Seattle, WA, USA, 1995.

[28] Daiheng Ni. A Unified Perspective on Traffic Flow Theory, Part II: The Unified Diagram. In *The proceedings of ASCE-ICCTP 2011 (Paper# 31)*, Nanjing, China, 2011. American Society of Civil Engineers.

[29] *Highway Capacity Manual*. Bureau of Public Roads, U.S. Dept. of Commerce, 1950.

[30] Nathan Gartner, Carroll J. Messer, and Ajay K. Rathi. *Revised Monograph of Traffic Flow Theory: A State-of-the-Art Report*. Transportation Research Board, 2001.

[31] J. M. Del Castillo. Three new models for the Flow-Density Relationship: Derivation and Testing for Freeway and Urban Data. *Transportmetrica, First published on: 30 March 2011 (iFirst). DOI: 10.1080/18128602.2011.556680*, 2011.

[32] B.D. Greenshields. A study of Traffic Capacity. *Proceedings of Highway Research Board*, 14:448–477, 1934.

[33] H. Greenberg. An Analysis of Traffic Flow. *Operations Research*, 7:78–85, 1959.

[34] J.S. Drake, J.L. Schofer, and A.D. May. A Statistical Analysis of Speed Density Hypotheses. *Highway Research Record*, 154:53–87, 1967.